Quantum reflection and interference of matter waves from periodically doped surfaces

Benjamin A. Stickler,[1,*] Uzi Even,[2] and Klaus Hornberger[1]
[1]*Faculty of Physics, University of Duisburg-Essen, Lotharstraße 1, 47048 Duisburg, Germany*
[2]*School of Chemistry, Tel Aviv University, Tel Aviv 69978, Israel*
(Received 27 October 2014; published 13 January 2015)

We show that periodically doped, flat surfaces can act as reflective diffraction gratings for atomic and molecular matter waves. The diffraction element is realized by exploiting the fact that charged dopants locally suppress quantum reflection from the Casimir-Polder potential. We present a general quantum scattering theory for reflection off periodically charged surfaces and discuss the requirements for the observation of multiple diffraction peaks.

DOI: 10.1103/PhysRevA.91.013614 PACS number(s): 03.75.Be, 34.35.+a, 37.25.+k, 03.65.Sq

I. INTRODUCTION

Quantum reflection refers to a nonvanishing reflection probability in the absence of a classical turning point [1–6]. It is a ubiquitous and inherently quantum-mechanical phenomenon relevant for chemical reactions, for the trapping of cold atoms in optical potentials, and for the scattering of atoms off surfaces [7–15].

Numerous theoretical works on quantum reflection of atoms and small particles can be found in the literature; more recent studies discuss the reflection of atoms from Casimir-Polder potentials [3,16,17], of antihydrogen from material slabs and nanoporous materials [18,19], and of small particles from evanescent laser fields [4,6]. Further works considered the case of temporally [20] and spatially [21] oscillating surfaces, and it was proposed that quantum reflection of photons from magnetic fields might even test nonlinearities of the quantum vacuum in strong fields [22].

Direct experimental observations of quantum reflection include the scattering of hydrogen atoms off superfluid helium [23], as well as reflection measurements of atoms from surfaces mediated by the long-range Casimir potential [5,10–12,24–27]. The use of periodically microstructured quantum reflection gratings enabled the detection of several diffraction orders [25,27]. Such optical elements can be attractive tools for metrological applications because diffraction gratings act as mass filters and because the reflection probability from the Casimir-Polder potential depends on the particle's polarizability [3]. For instance, the mass selective diffraction of a microstructured grating allowed direct observation of helium trimers [25]. The quantum reflection of Bose-Einstein condensates from a microstructured Fresnel mirror was numerically studied in [28].

Thus far, diffraction gratings for matter waves have been realized only with the help of periodic microstructures. These microstructures act mainly by physically blocking a part of the incoming wave, which is a purely geometrical effect [25]. It is a natural and open question whether quantum reflection gratings can also be realized without microstructured surfaces. It is the aim of this paper to answer this question in the affirmative and to demonstrate that quantum reflection into different diffraction orders can be realized with flat, periodically doped surfaces, thus circumventing the requirement for microstructures.

This paper is organized as follows: In Sec. II we discuss some general aspects of quantum scattering off periodic surfaces. The total interaction potential induced by periodically doped surfaces is then derived in Sec. III, where we also discuss its asymptotic behavior for $y \to \infty$. In Sec. IV we show that it suffices to consider this asymptotic form, and we investigate the associated specular reflection from the surface. Section V then demonstrates that periodically doped surfaces can be used as diffraction gratings, and we provide our conclusions in Sec. VI.

II. REFLECTION FROM PERIODIC SURFACE POTENTIALS

We consider the general quantum scattering problem of a small particle of mass m and static polarizability α off a perfectly planar but charged surface. The chosen coordinate system is as depicted in Fig. 1; that is, x and z are the in-plane coordinates, and the surface is situated at $y = 0$. The incoming beam is described by a plane wave $\psi_{\rm in}(\mathbf{r}) = \exp(i\mathbf{k}\cdot\mathbf{r})$, with $k_y < 0$. Denoting the angle of incidence by θ and the azimuthal angle by φ, we have the components of the initial wave vector $k_x = k\cos\theta\cos\varphi$, $k_y = -k\sin\theta$, and, $k_z = k\cos\theta\sin\varphi$. The angle θ is small in grazing incidence diffraction experiments, and hence, $k_x^2 + k_z^2 \gg k_y^2$, so that the energy of the lateral motion exceeds the energy of the motion towards the surface. Typically, θ is in the range $\theta \lesssim 20$ mrad [5,25,27].

In order to determine the reflection probability, we solve the Schrödinger equation,

$$(\Delta + k^2)\Psi(\mathbf{r}) - \frac{2m}{\hbar^2}V(\mathbf{r})\Psi(\mathbf{r}) = 0, \tag{1}$$

for the stationary scattering wave $\Psi(\mathbf{r})$ under appropriate boundary conditions as specified below. Here, $V(\mathbf{r})$ denotes the total interaction potential between the point particle and the surface; it will be discussed in detail in Sec. III.

If $V(\mathbf{r})$ is everywhere attractive, no classical turning point exists, although a finite reflectivity due to quantum reflection might occur. The concept of Wentzel-Kramers-Brillouin (WKB) wave functions proved to be particularly powerful for the theoretical description of quantum reflection [2]. This is due to the fact that the validity of the WKB approximation requires the local de Broglie wave length to

*benjamin.stickler@uni-due.de

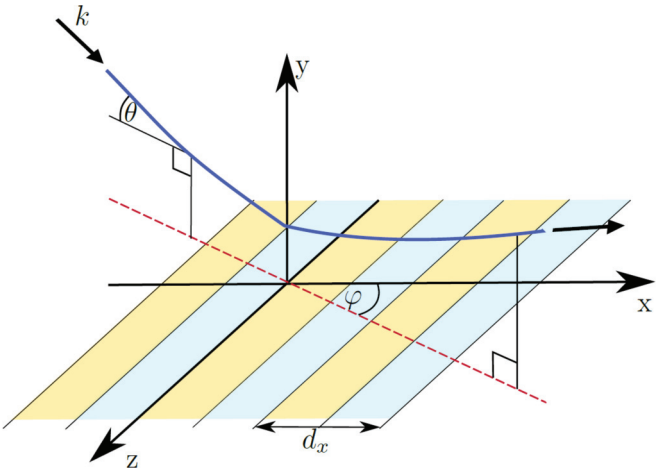

FIG. 1. (Color online) Schematic of the reflection problem. The incident wave vector **k** impinges with angle θ at the surface, and φ is the azimuthal angle with respect to the in-plane orientation.

vary sufficiently slowly [2,3,16], while a strong local variation of the de Broglie wave length indicates regions where quantum reflection is likely to occur. WKB waves are therefore the natural incoming and outgoing waves for quantum reflection problems. It is a remarkable general result that the WKB wave functions become exact for both large and small separations, $y \to \infty$ and $y \to 0$, if the interaction potential between the surface and the impinging particle vanishes faster than $1/y^2$ for large separations $y \to \infty$ [2]. The reflection probability then approaches unity in the limit of small normal velocities $k_y \to 0$. Moreover, if $V(\mathbf{r})$ is periodic, reflection into different diffraction orders is possible, as was observed experimentally with microstructured reflection gratings [25].

A. Boundary conditions

We proceed to specify the boundary conditions associated with Eq. (1) for $y \to \infty$ and $y \to 0$. For the time being, we restrict the discussion to potentials that vary periodically only in one in-plane direction, i.e., $V(\mathbf{r}) \equiv V(x,y) = V(x + a_x, y)$. This is done for the sake of simplicity; the generalization to potentials that are also periodic in the z direction is straightforward and will be briefly discussed at the end of this section.

Since the potential $V(x,y)$ is x periodic with period a_x and independent of z, the x component of the outgoing wave vector can differ only by integer multiples of the grating wave vector $q_x = 2\pi/a_x$, while the z component is preserved. The y component of the final momentum is determined by the conservation of total energy. Hence, the scattering state $\Psi(\mathbf{r})$ has the general asymptotic form

$$\Psi(\mathbf{r}) \overset{y\to\infty}{\longrightarrow} e^{i\mathbf{k}\cdot\mathbf{r}} + e^{ik_z z}\sum_{n\in\mathbb{Z}} r_n e^{i(k_x+nq_x)x} e^{ik_n y}, \tag{2}$$

with $k_n = \sqrt{k^2 - (k_x + nq_x)^2 - k_z^2}$ (which implies $k_0 = -k_y$). The reflection probability R_n into diffraction order n is given by $R_n = |r_n|^2$, and the total reflectivity is $R = \sum_n R_n$.

The second boundary condition, for $y \to 0$, depends on the specific behavior of the interaction potential $V(\mathbf{r})$ near the surface $y \to 0$. If $V(\mathbf{r})$ is proportional to C_γ/y^γ in this limit, independent of x and z, and if $\gamma > 2$, the WKB wave functions are exact near the surface [2]. It will become clear in Sec. III that the potential induced by a periodically doped surface meets this requirement due to the Casimir-Polder interaction, so that the second boundary condition can be stated as

$$\Psi(\mathbf{r}) \overset{y\to 0}{\longrightarrow} e^{ik_z z}\sum_{n\in\mathbb{Z}} t_n e^{i(k_x+nq_x)x}\psi^{(n)}_{\mathrm{WKB}}(y). \tag{3}$$

Here, the complex numbers t_n are transmission coefficients, and the outgoing WKB wave $\psi^{(n)}_{\mathrm{WKB}}(y)$ of order n is given by [2]

$$\psi^{(n)}_{\mathrm{WKB}}(y) = \frac{1}{\sqrt{p_n(y)}}\exp\left[-\frac{i}{\hbar}\int_{y_s}^{y} dy'\, p_n(y')\right], \tag{4}$$

where $p_n(y) = \sqrt{\hbar^2 k_n^2 - 2mC_\gamma/y^\gamma}$ is the local momentum for $y \to 0$ and y_s is some arbitrary starting point.

We remark that one can estimate whether or not the WKB wave function is a good approximation to the exact solution of the Schrödinger equation (1) by means of the badlands function [2]. In Sec. IV we will use the badlands function to estimate the reflection distance from the surface.

The stationary Schrödinger equation (1) together with the boundary conditions (2) and (3) states a well-posed boundary value problem which must be solved in order to obtain the reflection probabilities R_n. A more convenient formulation of the problem can be obtained by exploiting the periodicity of $V(x,y)$ in the in-plane direction x directly in the Schrödinger equation (1). The resulting equations, referred to as *coupled-channel equations*, replace Eq. (1) and will be derived next.

B. The coupled-channel equations

Since we assume for the moment that the interaction potential $V(x,y)$ is independent of the second in-plane coordinate z, the component k_z is preserved, and the stationary scattering wave $\Psi(\mathbf{r})$ can be expanded as

$$\Psi(\mathbf{r}) = e^{ik_z z}\sum_{n\in\mathbb{Z}} e^{i(k_x+nq_x)x}\psi_n(y). \tag{5}$$

Inserting this together with the Fourier decomposition $V(x,y) = \sum_n V_n(y)e^{inq_x x}$ into the Schrödinger equation (1) yields the coupled-channel equations [29],

$$\left(\partial_y^2 + k_n^2\right)\psi_n(y) - \frac{2m}{\hbar^2}\sum_{n'\in\mathbb{Z}} V_{n-n'}(y)\psi_{n'}(y) = 0. \tag{6}$$

These equations describe the coupling between different diffraction orders n with wave numbers $k_n = \sqrt{k^2 - (k_x + nq_x)^2 - k_z^2}$, which are linked by the Fourier coefficients $V_n(y)$ of the potential $V(x,y)$. Comparison with Eqs. (2) and (3) reveals that the boundary conditions to Eq. (6) are

$$\psi_n(y) \overset{y\to\infty}{\longrightarrow} \delta_{n0}e^{-ik_0 y} + r_n e^{ik_n y} \tag{7}$$

and

$$\psi_n(y) \overset{y\to 0}{\longrightarrow} t_n\psi^{(n)}_{\mathrm{WKB}}(y). \tag{8}$$

The coupled-channel equations (6) in combination with the boundary conditions (7) and (8) are the basis for the treatment

of quantum scattering and of quantum reflection off periodic surfaces. For a given interaction potential $V(x,y)$ one must, in general, resort to numerical methods. An algorithm for this task is presented in the Appendix.

Let us fix some notations which will be helpful when discussing general potentials. The diffraction order $n = 0$ is referred to as *specular*. Consequently, we refer to $V_0(y)$ as the *specular potential*, while $V_n(y)$, $n \neq 0$, is the nth *coupling potential*. Moreover, the wave number of the nth diffraction order k_n characterizes whether this diffraction order is *open* ($k_n^2 > 0$) or *closed* ($k_n^2 < 0$), in (imperfect) analogy to the notion of open and closed scattering channels in conventional scattering theory [30].

We remark that, in practice, it suffices to solve the coupled equations (6) only for the open diffraction orders, $k_n^2 > 0$. This is due to the fact that quantum reflection occurs far away from the surface where the influence of the closed-order wave functions is negligible (see [2,3,16] as well as Sec. IV).

The generalization of the coupled-channel equations (6) to a potential $V(\mathbf{r})$ which is periodic also in the z direction is straightforward and comes without any further complications [29]. In particular, a second Fourier index is added to all Fourier coefficients, and one must replace k_n with $k_{nm} = \sqrt{k^2 - (k_x + nq_x)^2 - (k_z + mq_z)^2}$. The resulting coupled-channel equations are then the direct generalization of Eqs. (6).

III. THE INTERACTION POTENTIAL

We now discuss the total interaction potential for a periodically doped surface and derive its asymptotic behavior. We will see in Sec. IV that its asymptotic shape determines the probability for quantum reflection and is thus of major significance for the observation of different diffraction orders.

The total interaction potential between a polarizable point particle and a doped surface consists of two contributions: (i) the Casimir-Polder (CP) interaction $V_{\mathrm{CP}}(y)$ and (ii) the electrostatic interaction $V_{\mathrm{el}}(\mathbf{r})$ induced by the surface charge $\sigma(x,z)$. The purely attractive CP interaction $V_{\mathrm{CP}}(y)$ between an atom and a flat surface can be well described with the aid of shape functions [2,3]. It behaves as $V_{\mathrm{CP}}(y) \to -C_4/y^4$ in the highly retarded limit $y \to \infty$, while it approaches $V_{\mathrm{CP}}(y) \to -C_3/y^3$ for small separations [31–33]. It is a matter of the particle and of the surface under investigation whether the highly retarded limit $y \to \infty$ suffices to describe quantum reflection [2].

Thus, the total interaction potential $V(\mathbf{r})$ can be written as

$$V(\mathbf{r}) = V_{\mathrm{CP}}(y) - \frac{\alpha}{2}|\mathbf{E}(\mathbf{r})|^2, \tag{9}$$

where the electrostatic field $\mathbf{E}(\mathbf{r})$ is determined by the surface charge distribution $\sigma(x,z)$,

$$\mathbf{E}(\mathbf{r}) = \frac{1}{4\pi\varepsilon_0}\int dx'dz' \frac{\sigma(x-x',z-z')}{(x'^2+y^2+z'^2)^{\frac{3}{2}}}\begin{pmatrix} x' \\ y \\ z' \end{pmatrix}. \tag{10}$$

The total interaction potential (9) is everywhere attractive; thus, no turning point exists. It falls off at least as $1/y^3$ near the surface $y \to 0$ due to the CP interaction, which justifies the use of WKB functions for small normal distances $y \to 0$ (see Sec. II and [2]). However, the asymptotic behavior assumed in (3) still requires that the potential (9) is independent of the in-plane coordinates x and z as $y \to 0$.

A. The electrostatic interaction potential

Let us therefore take a look at the electrostatic contribution $V_{\mathrm{el}}(\mathbf{r})$ to the total interaction potential (9) of the periodically doped surface. We exploit the periodicity of the doping by expanding the charge distribution $\sigma(x,z)$ as

$$\sigma(x,z) = \sum_{n\in\mathbb{Z}} \sigma_n(z) e^{in2\pi x/d_x}, \tag{11}$$

where d_x denotes the doping period (not necessarily equal to the period a_x of the potential). Naturally, we consider the case of an electrically neutral surface, $\sigma_0(z) = 0$, which avoids an infinitely extended constant electric field [34]. Moreover, for simplicity we assume that the charge distribution is symmetric in x, $\sigma(-x,z) = \sigma(x,z)$, and that it varies in the second in-plane direction z on a length scale much larger than the doping period d_x.

Inserting the Fourier decomposition (11) of $\sigma(x,z)$ into the expression for the electric field (10) and noting that the integrand is sharply peaked at $z' \simeq 0$, one obtains

$$\mathbf{E}(\mathbf{r}) \simeq \frac{1}{\varepsilon_0}\sum_{n=1}^{\infty} \sigma_n(z) e^{-n\kappa_x y}[\sin(n\kappa_x x)\mathbf{e}_x + \cos(n\kappa_x x)\mathbf{e}_y], \tag{12}$$

where we abbreviated $\kappa_x = 2\pi/d_x$. For large normal distances $y \gg 1/\kappa_x$, the electric field (12) decays exponentially on the length scale $1/\kappa_x = d_x/2\pi$, which is determined by the doping period d_x. This is due to the fact that the doping period d_x is the only length scale available in this system.

Inserting the field (12) into the total interaction potential (9) gives the electrostatic interaction potential $V_{\mathrm{el}}(\mathbf{r})$,

$$V_{\mathrm{el}}(\mathbf{r}) = -\frac{\alpha}{2\varepsilon_0^2}\left[\beta_0(y,z) + 2\sum_{n=1}^{\infty}\beta_n(y,z)e^{-n\kappa_x y}\cos(n\kappa_x x)\right], \tag{13}$$

where we introduced the coefficients

$$\beta_n(y,z) = \sum_{\ell=1}^{\infty}\sigma_\ell(z)\sigma_{\ell+n}(z)e^{-2\ell\kappa_x y}. \tag{14}$$

Importantly, in the asymptotic regime $y \gg 1/2\kappa_x$ the potential (13) also decays exponentially, however, on the length scale $1/2\kappa_x$, which is half the scale of the asymptotic electric field (12). The asymptotic shape of the electrostatic interaction potential (13) is thus completely determined by the doping period d_x, which is the only characteristic length in the problem. Since the electrostatic interaction decays exponentially for large normal distances y, the total interaction potential (9) decays asymptotically as $1/y^4$ due to the retarded CP potential, and hence, the reflectivity approaches unity for small normal velocities $k_0 \to 0$ [3].

The Fourier coefficients of the total interaction potential (9), as required in the coupled-channel equations (6), are easily obtained from of Eqs. (9) and (13). The specular potential

$V_0(y,z)$ reads

$$V_0(y,z) = V_{\rm CP}(y) - \frac{\alpha}{2\varepsilon_0^2}\sum_{\ell=1}^{\infty}\sigma_\ell^2(z)e^{-2\ell\kappa_x y}, \tag{15}$$

and the nth coupling potential takes on the form

$$V_n(y,z) = -\frac{\alpha}{2\varepsilon_0^2}\sum_{\ell=1}^{\infty}\sigma_\ell(z)\sigma_{\ell+|n|}(z)e^{-(2\ell+|n|)\kappa_x y}. \tag{16}$$

For example, a harmonic surface charge distribution in one in-plane direction, $\sigma(x,z) \equiv \sigma\cos(\kappa_x x)$ with Fourier coefficients $\sigma_\ell = \sigma\delta_{|\ell|1}/2$, yields $V_{\rm el}(\mathbf{r}) = -\alpha\sigma^2\exp(-2\kappa_x y)/8\varepsilon_0^2$. This potential is independent of the in-plane coordinate x; that is, it is purely specular, although the charge distribution is periodic. It is finite near the surface $y \to 0$, which implies that the CP potential dominates the total interaction potential for small y. Hence, the WKB wave functions $\psi^{(n)}_{\rm WKB}(y)$ for the CP potential become exact for $y \to 0$, as was presupposed in the boundary condition (3).

B. Asymptotic behavior of the specular interaction potential

It is a general result that the quantum reflection of a matter wave approaching the surface with a small velocity component in the normal direction is primarily influenced by the asymptotic tail of the attractive interaction potential [2,3]. It is easily verified by inspection of Eqs. (15) and (16) that the interaction potential (9) is asymptotically ($y \gg 1/2\kappa_x$) given by its specular interaction potential (15). At such distances from the surface the coupling to neighboring diffraction orders (16) is exponentially suppressed, and the x-specular potential $V_0(y,z)$ is, in leading order, given by

$$V_0(y,z) \simeq V_{\rm CP}(y) - \frac{\alpha}{2}\left(\frac{\sigma_1(z)}{\varepsilon_0}\right)^2 e^{-2\kappa_x y}. \tag{17}$$

As noted in the previous section, the asymptotic electrostatic potential (17) decays exponentially on the length scale $1/2\kappa_x = d_x/4\pi$ and is independent of the precise shape of the doping profile $\sigma(x,z)$ within the unit cell in the x direction.

We have thus seen that the CP interaction dominates the potential (17) at both close and far distances from the surface, $y \to 0$ and $y \to \infty$. This justifies the boundary conditions (3) also in the presence of the electrostatic interaction. In what follows, we focus on z-independent charge distributions, $\sigma_1 =$ const, for convenience, before returning to the general case $\sigma_1(z)$ in Sec. V.

If σ_1 is sufficiently large, an electrostatically dominated region exists between the CP region near the surface, $y \to 0$, and the CP region far above the surface, $y \to \infty$. In particular, for helium atoms and a given doping period d_x, this intermediate region exists for $\sqrt{\sigma_1}d_x \gtrsim e\sqrt{e_0}\sqrt[4]{3\pi}/2\sqrt[4]{4\alpha_{\rm f}}$, where $\alpha_{\rm f} = e_0^2/4\pi\varepsilon_0\hbar c$ is the fine-structure constant. This criterion can be obtained by equating the two different contributions of the x-specular potential (17) and minimizing in y. It must be emphasized that the criterion depends only on $\sqrt{\sigma_1}d_x$. For instance, for a doping period $d_x = 100$ nm, the required area density of carriers is roughly $\sigma_1/e_0 \gtrsim 5\times10^{15}$ electrons/m^2.

IV. REFLECTION DISTANCE AND SPECULAR QUANTUM REFLECTION

Within this section we first employ the maximum of the badlands function to estimate the reflection distance from the surface. We then demonstrate that periodically charged surfaces can suppress quantum reflection by calculating the reflection probabilities off a surface that is periodically doped in one in-plane direction. The reflection distance from the surface will justify the asymptotic approximation discussed in Sec. III.

A. Reflection distance from the surface

The badlands function $B(y)$ is an important tool for working with semiclassical wave functions since it indicates regions where the WKB approximation is a good estimate of the exact solution of the Schrödinger equation [2,3,16,17,35]. In particular, the WKB waves well approximate the exact wave function if the badlands function is small, $B(y) \ll 1$, while intervals where $B(y)$ is significantly nonzero can be regarded as regions where quantum reflection can occur [2,35]. Since no classical turning point exists in the potential (9), we use the maximum of the badlands function $B(y)$ to estimate the distance scale of quantum reflection.

The badlands function $B(y)$ is defined as [2]

$$B(y) = \hbar^2\left|\frac{3}{4}\frac{[p'(y)]^2}{[p(y)]^4} - \frac{p''(y)}{2[p(y)]^3}\right|, \tag{18}$$

where $p(y)$ is the local x-specular momentum (we still assume z independence in this section), i.e., $p(y) = \sqrt{\hbar^2k_0^2 - 2mV_0(y)}$, with $V_0(y)$ being the x-specular potential (17); the primes denote derivatives with respect to y.

If the total interaction potential is dominated by the CP interaction at all distances y, we may neglect the electrostatic contribution to the total potential (17). To keep the argument as simple as possible, we restrict the following discussion to the case in which the highly retarded limit $y \to \infty$ of the CP interaction is sufficient to describe quantum reflection, as it is the case, e.g., for helium atoms reflected from silica surfaces [2]. In this limit the CP potential is of the form $V_{\rm CP}(y) = -C_4/y^4$, with $C_4 = 3\hbar c\alpha/32\pi^2\varepsilon_0$ [31], and the maximum of the badlands function is approximately at

$$y_{\rm CP} = \frac{1}{\sqrt{v_0\sin\theta}}\sqrt[4]{\frac{3\hbar c}{16\pi^2\varepsilon_0}\frac{\alpha}{m}}, \tag{19}$$

above the surface. The scale of the reflection distance is thus in this case determined completely by the properties of the particle and independent of the doping period d_x and charge density σ_1. Moreover, since the reflection distance depends only on the ratio between polarizability and mass, α/m, it is approximately the same for atomic clusters of arbitrary size. However, the reflection probability decreases with increasing cluster size [2].

On the other hand, if the electrostatic contribution dominates the quantum reflection, the maximum of the badlands function lies approximately at

$$y_{\rm el} = \frac{d_x}{4\pi}\ln\left[\frac{64\pi^3\alpha_{\rm f}}{3(5-\sqrt{21})}\frac{\sigma_1^2}{e_0^2}y_{\rm CP}^4\right], \tag{20}$$

above the surface. The reflection distance then increases linearly with the doping period d_x and depends only logarithmically on the charge density σ_1 and the CP reflection length scale y_{CP}.

For example, helium atoms approaching the surface with an initial velocity of $v_0 \simeq 300$ m s^{-1} at an incidence angle $\theta \geqslant 1$ mrad have a CP reflection distance of $y_{\mathrm{CP}} \lesssim 40$ nm above the surface. For an exemplary charge-carrier density $\sigma_1/e_0 \simeq 10^{16}$ electrons/m^2 the maximum of the badlands function (20) is then at a position $y_{\mathrm{el}} > 1/2\kappa_x = d_x/4\pi$, which is deep in the asymptotic regime of the electrostatic interaction potential (13). This justifies the specular approximation of the total interaction potential (17) for this charge density.

In fact, it can be argued that the asymptotic approximation (17) is sufficient to describe quantum reflection for arbitrary charge densities σ_1. For large densities it is valid due to the mentioned large reflection distances (20), while for small densities the reflectivity from the purely electrostatic interaction potential tends towards zero (for the exact and for the asymptotic electrostatic interactions). The physical reason for the latter is that in the case of small doping periods d_x the electric field can be neglected because the CP potential dominates the total interaction potential (17); on the other hand, in the case of large d_x the reflection probability approaches zero, as will be shown in the next section.

B. Specular quantum reflection

We now explicitly calculate the probability for quantum reflection from a flat surface that is periodically charged with period d_x in one in-plane direction. This requires solving the Schrödinger equation (1) with the asymptotic interaction potential (17) for $\sigma_1 = \text{const}$. It can be seen from the coupled-channel equations (6) that this is equivalent to solving these equations only for the isolated specular channel,

$$\left(\partial_y^2 + k_0^2\right)\psi_0(y) - \frac{2m}{\hbar^2} V_0(y)\psi_0(y) = 0, \tag{21}$$

with the specular boundary conditions (7) and (8) ($n = 0$).

If the interaction potential is dominated by the CP interaction for all normal distances y, the reflection probability can be obtained in leading order from zero-energy solutions of Eq. (21) [16]. It then tends towards unity for decreasing normal velocity $k_0 \to 0$ and decreases, in the highly retarded limit, for increasing values of the characteristic CP length $b_{\mathrm{CP}} = \sqrt{2mC_4}/\hbar$ [2].

On the other hand, if the interaction potential has a dominantly electrostatic region, Eq. (6) describes reflection from an exponential quantum well and can be solved analytically (since substitution $\xi \propto e^{-\kappa_x y}$ turns Eq. (21) into a Bessel differential equation of complex-order) [1,4]. In this case the total reflection probability R is [4]

$$R = e^{-k_0 d_x}. \tag{22}$$

The reflection probability tends towards unity for vanishing normal velocities $k_0 \to 0$ and decreases with increasing doping period d_x. The physical reason is that for a given doping period d_x the asymptotic electric field (12), and therefore also the asymptotic interaction potential (13), decays exponentially on the scale defined by the period d_x. In the limit of large d_x the asymptotic electrostatic potential (17) decays slowly, and thus, the probability for quantum reflection tends to zero.

Returning to the discussion of the length scale (20) of quantum reflection, we now see that it is, indeed, hardly possible to observe different diffraction orders if the charge density is periodic only in the x direction. The reason is that for a significant coupling between the x channels the surface charge has to be small because of Eq. (20). This in turn requires large doping periods d_x, implying low reflection probabilities (22). However, one can create grating structures by locally suppressing quantum reflection in a controlled fashion, as we discuss next.

V. QUANTUM REFLECTION INTO DIFFERENT DIFFRACTION ORDERS

In the previous section we saw that if the surface charge $\sigma(x,z)$ is periodic in a single in-plane direction x, its period d_x defines the dominant length scale of the system. This length scale then determines the probability of quantum reflection (22), implying that the coupling to different diffraction orders is suppressed.

Thus, to observe diffraction into different diffraction orders a second length scale has to be introduced. This is most easily achieved by making the surface charge density $\sigma(x,z)$ periodic also in the second in-plane direction z. (Alternatively, one can think of a one-dimensional superstructure with two different periods.) We then deal with a two-dimensional periodic surface charge $\sigma(x,z)$ inducing the electric field which attracts the impinging particle. Again, the reflection probability is determined by the asymptotic shape of the electrostatic interaction potential in the normal direction y. It follows from Eq. (12) that if the period d_z in one in-plane direction is much greater than the period d_x in the other in-plane direction, $d_z \gg d_x$, the asymptotic electric field decays on the length scale set by the smaller period d_x, while the z dependence of the surface charge $\sigma_1(z)$ determines the amplitude of the asymptotic field (12). At positions z where the charge $\sigma_1(z)$ is large, quantum reflection can be suppressed according to the discussion of the previous section, while at positions z where $\sigma_1(z)$ is close to zero, CP reflection can occur. In this way it is possible to realize a reflective diffraction grating in the direction z consisting of an alternating sequence of absorptive "grating bars" and reflective regions in between. Each absorptive grating bar is realized by short-period doping in the x direction perpendicular to the grating direction z.

A. Theoretical description

We thus consider a two-dimensional periodic surface charge density $\sigma(x,z)$ with periods d_x and d_z, with a small ratio $d_x/d_z \ll 1$ so that the asymptotic electric field (12) in the normal direction is determined by d_x. The asymptotic behavior of the total interaction potential is then given by the specular potential (17), where the charge modulation $\sigma_1(z)$ is now allowed to be a periodic function of the grating direction z. The asymptotic total potential (17) is independent of the in-plane coordinate x, making k_x a preserved quantity. Moreover, the potential decays exponentially in the normal direction with the length scale set by the smaller period d_x. If the charge

modulation $\sigma_1(z)$ varies smoothly with period d_z between zero and some finite value σ_m, one observes, alternatingly, regions where quantum reflection can occur from the CP potential [$\sigma_1(z) \simeq 0$] and regions where quantum reflection is suppressed due to the presence of the electrostatic interaction [$\sigma_1(z) \simeq \sigma_m$].

To describe the probability of reflection off this diffraction grating, we solve the stationary Schrödinger equation (1) for the specular potential (17),

$$\left(\partial_y^2 + \partial_z^2\right)\psi(y,z) - \frac{2m}{\hbar^2}V_0(y,z)\psi(y,z) = 0, \tag{23}$$

where the total scattering state is $\Psi(\mathbf{r}) = e^{ik_x x}\psi(y,z)$. Repeating the steps described in Sec. II yields the coupled-channel equations for the diffraction in the z direction in direct analogy to Eqs. (6). They can be solved numerically with the algorithm explained in the Appendix.

To demonstrate the working principle of the diffraction grating it suffices to regard an initial wave packet approaching the surface along the short-period in-plane direction x. Thus, we have $\varphi = 0$ and $k_z = 0$. This means that the asymptotically outgoing diffraction orders have in-plane momentum $k_z' = nq_z$, where $q_z = 2\pi/a_z$ denotes the lattice wave number in the z direction, while the normal component k_y changes to $k_n = \sqrt{k^2 - k_x^2 - (nq_z)^2}$ according to the conservation of energy. Since $k_z = 0$, the expected diffraction pattern is symmetric, $R_n = R_{-n}$.

For long grating periods $d_z \gg d_x$ it is natural to assume that $2\pi/d_z k_0 \ll 1$, which is usually known as the sudden approximation [29]. This means that all outgoing waves have approximately the same wave number, $k_n \simeq k_0$. Then the Schrödinger equation (23) simplifies to

$$\left(\partial_y^2 + k_0^2\right)\psi(y,z) - \frac{2m}{\hbar^2}V_0(y,z)\psi(y,z) = 0. \tag{24}$$

Here, the grating direction z enters the equation only in a parametric fashion, and hence, the scattering state $\psi(y,z)$ also depends on z only parametrically. The corresponding asymptotic boundary condition (2) can be expressed as

$$\psi(y,z) \overset{y\to\infty}{\longrightarrow} e^{-ik_0 y} + r(z)e^{ik_0 y}. \tag{25}$$

In general, the resulting reflection probability is a function of the grating direction z, $R(z) = |r(z)|^2$, and the probability of diffraction into the nth order $R_n = |r_n|^2$ is obtained from

$$r_n = \frac{1}{a_z}\int_{-\frac{a_z}{2}}^{\frac{a_z}{2}} dz r(z)e^{-inq_z z}. \tag{26}$$

It is easily verified that $R = (1/a_z)\int_{-a_z/2}^{a_z/2} dz R(z)$ is the total reflectivity.

In order to discuss particular examples we rewrite the Schrödinger equation (24) by defining the dimensionless periodic function $\Delta(z)$ by $\sigma_1(z) = \sigma_m\Delta(z)$, where $\sigma_m = \text{const}$ is the doping amplitude. Hence, the nth-order coupling potential $V_n(y)$ between diffraction orders in the grating direction z is given by

$$V_n(y) = -\frac{\alpha}{2a_z}\left(\frac{\sigma_m e^{-\kappa_x y}}{\varepsilon_0}\right)^2 \int_{-\frac{a_z}{2}}^{\frac{a_z}{2}} dz \Delta^2(z)e^{-inq_z z}. \tag{27}$$

B. Stripe geometry

As a first example we discuss the case where the grating bars are of the form of rectangular doping stripes in grating direction z,

$$\Delta(z) = \sum_{n\in\mathbb{Z}} \Theta\left(\frac{f d_z}{2} - |z - nd_z|\right). \tag{28}$$

Here, $f \in [0,1)$ is the opening fraction of the grating. Clearly, in this case $\Delta(z)$ is not slowly varying in the direction of the grating z so that the validity of the asymptotic interaction potential (17) is questionable; however, we ignore this for the moment.

We solve the Schrödinger equation (24) for all positions z in the grating direction. If z is within the grating bar, $\Delta(z) = 1$, the reflection coefficient vanishes approximately, $r(z) = 0$, because quantum reflection is suppressed by the electrostatic interaction. On the other hand, at positions z where $\Delta(z) = 0$, the reflection coefficient is close to the value of pure CP reflection of a flat surface, $r(z) \simeq r_{CP}$. In summary, we obtain

$$r(z) = r_{CP}[1 - \Delta(z)], \tag{29}$$

and the probability for reflection into the nth diffraction order $R_n = |r_n|^2$ reads

$$R_n = R_{CP}(1-f)^2\text{sinc}^2[n(1-f)\pi], \tag{30}$$

with $R_{CP} = |r_{CP}|^2$. This is exactly the diffraction intensity expected from a periodic grating with opening fraction $(1-f)$ [36].

In addition, we note that the total reflectivity R is given by $R = (1-f)R_{CP}$; that is, it depends on the properties of the impinging particle through R_{CP}. In particular, denoting by b_{CP} the characteristic length of the CP potential, the CP reflection probability R_{CP} approaches unity for $k_0 b_{CP} \to 0$, and it decreases exponentially with increasing $k_0 b_{CP}$ [2]. If the CP length scale b_{CP} is dominated by the highly retarded limit, $b_{CP} = \sqrt{2mC_4}/\hbar$ [2], the reflectivity decreases exponentially with $v_0 \sin\theta\sqrt{\alpha m}$.

We compare the analytic result (30) with the exact, numerically obtained reflectivities for helium atoms with the initial velocity $v_0 = 300$ m s^{-1}, approaching the surface at incidence angle $\theta = 1$ mrad. The short doping period is $d_x = 500$ nm, while the long doping period is $d_z \simeq 40$ μm; the doping amplitude is set to $\sigma_m/e_0 = 10^{16}$ electrons/m^2, and the grating fraction is given by $f = 1/2$. The coupled-channel equations (6) are solved numerically with the help of Johnson's log-derivative method (see the Appendix). The coupling potentials $V_n(y)$ which appear in the coupled-channel equations (6) are given by

$$V_n(y) = -\frac{\alpha f}{2}\left(\frac{\sigma_m e^{-\kappa_x y}}{\varepsilon_0}\right)^2 \text{sinc}(nf\pi). \tag{31}$$

The probability R_{CP} for flat CP reflection required in (30) is calculated numerically with the help of the same method.

In Fig. 2(a) we see agreement between the numerically obtained diffraction probabilities and the analytically approximated values (30). In particular, while the specular peak is slightly overestimated by (30), the reflection probabilities for the first diffraction orders are well described. This example

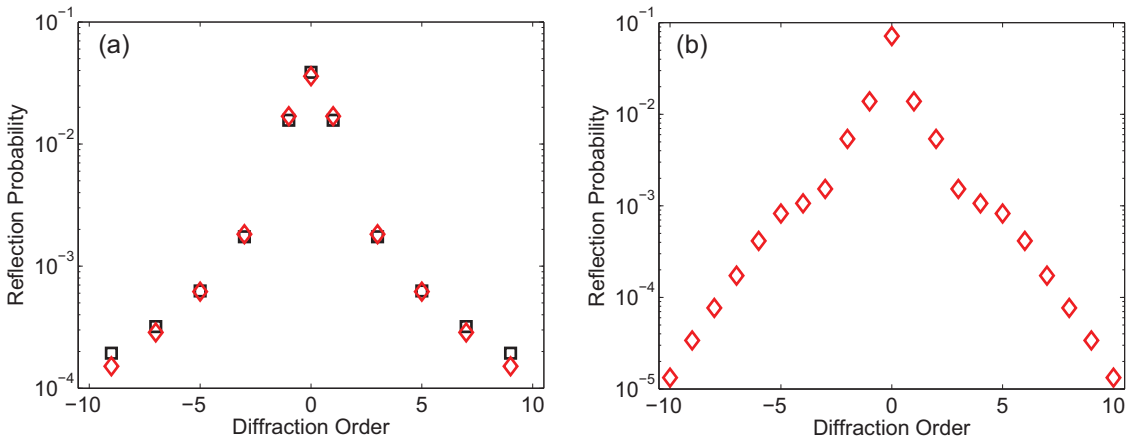

FIG. 2. (Color online) Probabilities of reflection into different diffraction orders for a doping profile $\Delta(z)$ given by (a) Eq. (28) and (b) Eq. (32). In (a) the numerically obtained values (red diamonds) compare well with the analytical result (black squares) given by Eq. (30).

clearly shows that the flat diffraction grating can be realized with the help of two-dimensional periodic surface doping.

More complicated doping structures $\Delta(z)$ can only be treated by solving the coupled-channel equations (6) numerically. As a second example, we investigate the diffraction pattern resulting from a Gaussian doping profile, which might be much more realistic. Specifically, the doping profile $\Delta(z)$ is of the form

$$\Delta(z) = \sum_{k\in\mathbb{Z}} \exp\left(-\frac{(z-kd_z)^2}{2\varepsilon^2}\right), \tag{32}$$

where we assume that the width $\varepsilon \ll d_z$ so that there is negligible overlap between neighboring grating bars. The coupling potentials $V_n(y)$ are then of the form

$$V_n(y) = -\frac{\alpha\varepsilon\sqrt{\pi}}{2d_z}\left(\frac{\sigma_m e^{-\kappa_x y}}{\varepsilon_0}\right)^2 \exp\left[-\left(\frac{n\varepsilon\pi}{d_z}\right)^2\right]. \tag{33}$$

The diffraction pattern is shown in Fig. 2(b) for helium atoms. The parameters are as above, except the doping amplitude is $\sigma_m/e_0 = 10^{15}$ electrons/m^2; the width of the doping profile is $\varepsilon = d_z/10$. Again, we find that the observation of multiple diffraction peaks is clearly possible. Compared with the previous example, the reflection probability of the specular peak is enhanced, while the probabilities of reflection into the first diffraction orders are of a comparable magnitude.

VI. CONCLUSION

We demonstrated that quantum reflection of atomic and molecular matter waves into multiple diffraction orders can be achieved with flat, periodically charged surfaces. The electric field generated by the surface dopants provides a force in addition to the Casimir-Polder interaction that can locally suppress quantum reflection. Diffraction into different orders is then achievable with a two-dimensional doping pattern that is periodic in both surface directions. The diffraction grating consists of an alternating sequence of absorptive grating bars and reflective "grating slits," where each grating bar is realized by periodic surface doping. The quantum reflection occurs from the Casimir-Polder potential in the grating slits, i.e., in undoped regions between two neighboring grating bars. The reflection probabilities are comparable in magnitude and scaling to previous diffraction experiments off the Casimir-Polder interaction of microstructured gratings. Mass selection and the observation of multiple diffraction peaks should thus be possible also with flat, doped surfaces.

In this work we have developed a quantum theory of scattering of matter waves from periodically charged surfaces. The investigation of quantum reflection from a surface which is periodically doped only in one in-plane direction revealed that the reflectivity can be efficiently suppressed. This is due to the fact that the asymptotic shape of the electrostatic interaction potential is fixed by the doping period d_x. It was argued, by estimating the reflection distance from the surface, that in this case the asymptotic interaction potential suffices completely to describe quantum reflection. Moreover, the asymptotic shape of the interaction potential was found to be independent of the specific doping structure, so that the coupling to different diffraction orders is suppressed if the surface doping is periodic in only a single in-plane direction. Based on this observation we proposed realizing flat diffraction gratings for matter waves with a two-dimensional grating-like structure. We determined the diffraction intensities for helium atoms and demonstrated that the observation of several diffraction peaks is, indeed, possible. This makes the discussed setup an alternative to microstructured matter-wave diffraction elements.

A natural question is whether the idea of modulating the reflection by periodic doping can be extended to realize further flat optical elements, such as flat concave mirrors or Fresnel mirrors, by appropriately adjusting the surface doping. Such optical elements for quantum reflection may well be easier to produce than their microstructured counterparts since the asymptotic form of the interaction potential is independent of the precise doping structure within the absorptive bars.

ACKNOWLEDGMENTS

We thank A. R. Barnea for helpful discussions, and we acknowledge support from the European Commission within NANOQUESTFIT (Grant No. 304886).

APPENDIX: NUMERICAL METHOD

To solve the coupled-channel equations (6) (where n labels x- or z-diffraction orders) we employ Johnson's log-derivative method [37]. It is based on formulating Eq. (6) as a matrix equation for the matrix $\mathbf{\Psi}(y) = [\Psi_{nm}(y)]$, where $\Psi_{nm}(y)$ denotes the nth component of the mth solution vector associated with incident momentum k_m. Hence, the matrix elements of interest are $\Psi_{n0}(y)$ with incident momentum k_0. Defining the logarithmic derivative matrix $\mathbf{Z}(y) = \mathbf{\Psi}'(y)\mathbf{\Psi}^{-1}(y)$ gives a matrix Riccati equation

$$\mathbf{Z}'(y) + \mathbf{Z}^2(y) + \mathbf{U}(y) = \mathbf{0}, \tag{A1}$$

with the potential matrix $\mathbf{U}(y)$ defined as

$$U_{nm}(y) = k_n^2\delta_{nm} - \frac{2m}{\hbar^2}V_{n-m}(y). \tag{A2}$$

Since the badlands function $B(y)$ vanishes for $y \to 0$ (see Sec. III), we know that in this limit $\mathbf{Z}(y)$ is well approximated by the WKB solution with $V(y) \simeq V_{\mathrm{CP}}(y)$. Therefore, $\mathbf{Z}(y)$ is given by, for $y \to 0$,

$$\mathbf{Z}(y) \xrightarrow{y\to 0} \mathrm{diag}\left[-\frac{i}{\hbar}p_n(y) - \frac{p_n'(y)}{2p_n(y)}\right], \tag{A3}$$

where $p_n(y) = \sqrt{\hbar^2k_n^2 - 2mV_{\mathrm{CP}}(y)}$ is the local momentum of the nth diffraction order. The WKB solution (A3) is then propagated with the help of Johnson's algorithm [37] towards $y \to \infty$, where, again, the badlands function vanishes. The reflection matrix $\mathbf{R}$ is then identified by matching $\mathbf{Z}$ to

$$\mathbf{\Psi}(y) \simeq \exp(-i\mathbf{K}y) + \exp(i\mathbf{K}y)\mathbf{R}, \tag{A4}$$

where $\mathbf{K} = \mathrm{diag}(k_n)$. In particular, we calculate

$$\mathbf{R} = \exp(-i\mathbf{K}y)[(i\mathbf{K} - \mathbf{Z})^{-1}(i\mathbf{K} + \mathbf{Z})]\exp(-i\mathbf{K}y), \tag{A5}$$

which is independent of y for $y \to \infty$. The reflection coefficients r_n are the entries of R_{n0}.

The algorithm is as follows [37]: Let M be the even number of equidistant grid points, $y_m = y_0 + m\Delta y$, where, in our case, $y_0 = 0$ and $\Delta y = y_{\mathrm{end}}/M$, and let $\mathbf{U}_m = \mathbf{U}(y_m)$. The matrix is initialized with

$$\mathbf{Y}_0 = \mathbf{Z}(0) - \frac{\Delta y}{3}\mathbf{U}_0 \tag{A6}$$

and is propagated in two steps,

$$\mathbf{Y}_{m+1} = (\mathbf{I} + \Delta y\mathbf{Y}_m)^{-1}\mathbf{Y}_m - \frac{4\Delta y}{3}\left(\mathbf{I} + \frac{\Delta y^2}{6}\mathbf{U}_{m+1}\right)^{-1}\mathbf{U}_{m+1} \tag{A7}$$

and

$$\mathbf{Y}_{m+2} = (\mathbf{I} + \Delta y\mathbf{Y}_{m+1})^{-1}\mathbf{Y}_{m+1} - \frac{2\Delta y}{3}\mathbf{U}_{m+2}. \tag{A8}$$

Finally, in the last step Eq. (A8) is replaced by

$$\mathbf{Z}(y_{\mathrm{end}}) \equiv \mathbf{Y}_M = (\mathbf{I} + \Delta y\mathbf{Y}_{M-1})^{-1}\mathbf{Y}_{M-1} - \frac{\Delta y}{3}\mathbf{U}_M. \tag{A9}$$

The error decreases as $O(h^4)$ [37].

[1] L. Landau and E. Lifschitz, *Lehrbuch der Theoretischen Physik III: Quantenmechanik* (Akademie, Berlin, 1988).
[2] H. Friedrich and J. Trost, Phys. Rep. **397**, 359 (2004).
[3] H. Friedrich, G. Jacoby, and C. G. Meister, Phys. Rev. A **65**, 032902 (2002).
[4] C. Henkel, C. I. Westbrook, and A. Aspect, J. Opt. Soc. Am. B **13**, 233 (1996).
[5] B. S. Zhao, H. C. Schewe, G. Meijer, and W. Schöllkopf, Phys. Rev. Lett. **105**, 133203 (2010).
[6] B. Segev, R. Côté, and M. G. Raizen, Phys. Rev. A **56**, R3350 (1997).
[7] R. S. Friedman and D. G. Truhlar, Chem. Phys. Lett. **183**, 539 (1991).
[8] R. Friedman and M. Jamieson, Comput. Phys. Commun. **85**, 231 (1995).
[9] A. Jurisch and J.-M. Rost, Phys. Rev. A **77**, 043603 (2008).
[10] F. Shimizu, Phys. Rev. Lett. **86**, 987 (2001).
[11] T. A. Pasquini, Y. Shin, C. Sanner, M. Saba, A. Schirotzek, D. E. Pritchard, and W. Ketterle, Phys. Rev. Lett. **93**, 223201 (2004).
[12] T. A. Pasquini, M. Saba, G.-B. Jo, Y. Shin, W. Ketterle, D. E. Pritchard, T. A. Savas, and N. Mulders, Phys. Rev. Lett. **97**, 093201 (2006).
[13] W. Brenig, Z. Phys. B Condens. Matter **36**, 227 (1980).
[14] J. Böheim, W. Brenig, and J. Stutzki, Z. Phys. B Condens. Matter **48**, 43 (1982).
[15] W. Brenig and R. Russ, Surf. Sci. **278**, 397 (1992).
[16] R. Côté, H. Friedrich, and J. Trost, Phys. Rev. A **56**, 1781 (1997).
[17] C. Eltschka, M. J. Moritz, and H. Friedrich, J. Phys. B **33**, 4033 (2000).
[18] G. Dufour, A. Gérardin, R. Guérout, A. Lambrecht, V. V. Nesvizhevsky, S. Reynaud, and A. Y. Voronin, Phys. Rev. A **87**, 012901 (2013).
[19] G. Dufour, R. Guérout, A. Lambrecht, V. V. Nesvizhevsky, S. Reynaud, and A. Y. Voronin, Phys. Rev. A **87**, 022506 (2013).
[20] B. Herwerth, M. DeKieviet, J. Madroñero, and S. Wimberger, J. Phys. B **46**, 141002 (2013).
[21] D. Kouznetsov and H. Oberst, Phys. Rev. A **72**, 013617 (2005).
[22] H. Gies, F. Karbstein, and N. Seegert, New J. Phys. **15**, 083002 (2013).
[23] J. J. Berkhout, O. J. Luiten, I. D. Setija, T. W. Hijmans, T. Mizusaki, and J. T. M. Walraven, Phys. Rev. Lett. **63**, 1689 (1989).
[24] V. Druzhinina and M. DeKieviet, Phys. Rev. Lett. **91**, 193202 (2003).
[25] B. S. Zhao, S. A. Schulz, S. A. Meek, G. Meijer, and W. Schöllkopf, Phys. Rev. A **78**, 010902 (2008).
[26] H. C. Schewe, B. S. Zhao, G. Meijer, and W. Schöllkopf, New J. Phys. **11**, 113030 (2009).
[27] B. S. Zhao, W. Zhang, and W. Schöllkopf, Mol. Phys. **111**, 1772 (2013).

[28] T. E. Judd, R. G. Scott, G. Sinuco, T. W. A. Montgomery, A. M. Martin, P. Krüger, and T. M. Fromhold, New J. Phys. **12**, 063033 (2010).
[29] J. Manson, in *Helium Atom Scattering from Surfaces*, edited by E. Hulpke, Springer Series in Surface Sciences Vol. 27 (Springer, Berlin, 1992), pp. 173–205.
[30] J. Taylor, *Scattering Theory: The Quantum Theory of Nonrelativistic Collisions* (Dover, Mineola, NY, 2000).
[31] S. Y. Buhmann and D.-G. Welsch, Prog. Quantum Electron. **31**, 51 (2007).
[32] S. Y. Buhmann, *Dipsersion Forces I: Macroscopic Quantum Electrodynamics and Ground-State Casimir, Casimir-Polder and van der Waals Forces* (Springer, Berlin, 2012).
[33] S. Y. Buhmann, *Dipsersion Forces II: Many-Body Effects, Excited Atoms, Finite Temperature and Quantum Friction* (Springer, Berlin, 2012).
[34] J. Jackson, *Classical Electrodynamics* (Wiley, New York, 1999).
[35] A. Jurisch and H. Friedrich, Phys. Rev. A **70**, 032711 (2004).
[36] M. Born and E. Wolf, *Principles of Optics* (Cambridge University Press, Cambridge, 2013).
[37] B. Johnson, J. Comput. Phys. **13**, 445 (1973).